Analysis of the Nonlinear Rolling Motion of Finned Missiles

CHARLES J. COHEN,* THOMAS A. CLARE,† AND FRANK L. STEVENS‡
Naval Weapons Laboratory, Dahlgren, Va.

A method is presented for applying "global" nonlinear least squares procedures to the differential equation describing the nonlinear (roll lock-in, break-out and speed-up) rolling motion of finned missiles at high angles of attack. The method consists of 1) segmenting the data with constant aerodynamics fitting for the initial conditions of each segment; then 2) "globally" fitting one set of aerodynamic coefficients for all segments and initial conditions of each segment. Nonlinear aerodynamic coefficients, extracted from data taken on a basic research configuration at an angle of attack of 57°, are presented and discussed regarding their impact on observed roll behavior.

Nomenclature

A = reference area, ft^2
C_{jk} = roll moment coefficient, defined in Eq. (1)
d = reference length, ft
I_x = axial moment of inertia, slug-ft^2
n = total number of segments
p = rolling velocity, rad/sec
Q = dynamic pressure, $1/2\ V^2$, lb/ft^2
$\mathbf{Q}$ = QAd/I_x
S_{jk} = roll moment coefficient, defined in Eq. (1)
t = time, sec
V = velocity, fps
α = angle of attack, rad or deg
γ = roll orientation angle computed by Eq. (1), rad or deg
δ_A = fin cant, rad or deg
$\dot{(\ )}$ = $d(\ )/dt$
$(\ )^T$ = transpose of ( )
$(\ )^{-1}$ = inverse of ( )
$(\ )^a$ = corresponds to aerodynamic coefficients
$(\ )^j$ = corresponds to initial conditions of the jth segment

Introduction

THE rolling motion of finned bodies has been shown[1,2] to be described by several basic roll phenomena labeled "linear" rolling motion, roll "slow-down," roll "lock-in," roll "break-out" and roll "speed-up." These are basically a function of angle of attack, with the aforementioned phenomena occurring with increasing angle of attack. Figure 1 schematically describes these regions of roll behavior in a steady-state fashion.

The stability characteristics of finned bodies, e.g., bombs, rockets, missiles, are critically dependent on the vehicle's roll behavior. Bombs, for example, must be spun intentionally to avoid large dispersion due to manufacturing tolerances. Design spin rates cannot be too large, however, without introducing the possibility of Magnus instability. Consequently, the design fin cant (including tolerances) sometimes produces lower than intended roll rates and permits, by the action of the induced roll and side moments, roll-yaw coupling; high angles of attack result. Depending on the fin/body configuration, stronger lock-in or roll speed-up could develop, the latter inducing spin rates far in excess of design values. The increased Magnus moments would then provide significantly reduced damping; and closure of the angle of attack envelope becomes severely impeded. Furthermore, guided missiles, which may be subject to a wide angle of attack range, must be capable of enduring large differences in roll aerodynamics, whether roll controlled or not.

It is, therefore, necessary to have some neans for analyzing and predicting rolling motion at high angles of attack, in the hope of alleviating these phenomena[3] or including them in design considerations. Differential equations of motion and methods of extracting aerodynamic coefficients from roll behavior in the linear, slow-down, and lock-in regions have been developed.[4,5] A description of all phases of the nonlinear rolling motion has recently been given[6]: a nonlinear, second-order differential equation of motion was presented which was shown to be capable of describing the various roll phenomena separately, or in combination.

High order, nonlinear roll moment coefficients, which were not amenable to direct measurement experimentally (strain gage, steady-state spin, etc.), were introduced to predict this roll behavior. It was felt that application of nonlinear least squares principles[7] toward fitting the equation of motion to observed,

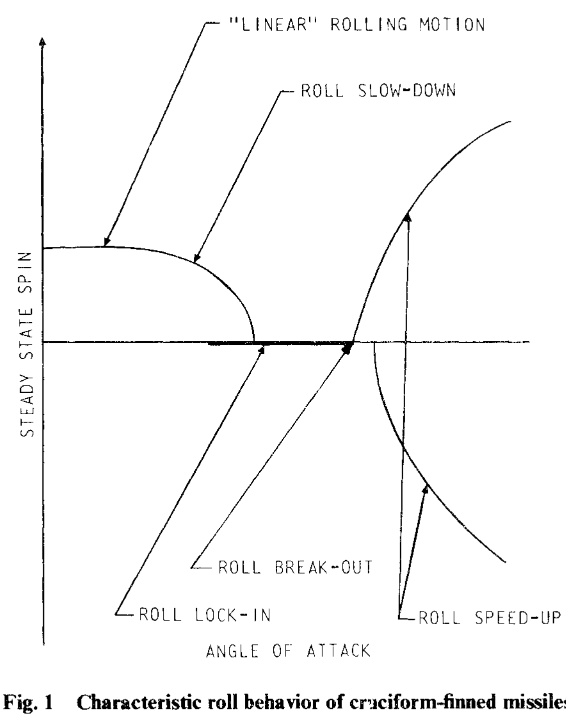

Fig. 1 Characteristic roll behavior of cruciform-finned missiles.

Presented as Paper 72-980 at the AIAA 2nd Atmospheric Flight Mechanics Conference, Palo Alto, Calif., September 11–13, 1972; submitted July 18, 1973; revision received October 17, 1973.

Index categories: LV/M Aerodynamics; LV/M Dynamics, Uncontrolled.

* Research Associate, Warfare Analysis Department.
† Research Scientist, Warfare Analysis Department. Member AIAA.
‡ Aerospace Engineer, Warfare Analysis Department. Associate Member AIAA.

dynamic roll angular data would lead to measurement of these coefficients. Nonlinear least squares procedures, however, require initial estimates of the parameters (or coefficients) to be determined. The severely nonlinear nature of the differential equation and the observed data, in addition to limited knowledge of most nonlinear coefficients, requires some modification to standard procedures in order to achieve convergence of fit on a repeatable basis.

Therefore, the purpose of this paper is to present a method for applying nonlinear least squares to such an equation. The paper describes the method and the equations pertinent to its application. The technique is applied to subsonic roll angular data taken on a basic research missile at an angle of attack of 57°. Resultant aerodynamic coefficients are presented and discussed regarding their impact on observed roll behavior. Roll angular data were also analyzed for other angles of attack; these are discussed in Ref. 12.

Equation of Motion

The following differential equation of motion is suitable to accurately describe the rolling motion of symmetric cruciform-finned missiles[6]

$$\ddot{\gamma} = \mathbf{Q} \sum_{j=0}^{\infty} \left(\frac{\dot{\gamma} d}{2V}\right)^j \sum_{k=0}^{\infty} (C_{jk} \cos 4k\gamma + S_{jk} \sin 4k\gamma) \tag{1}$$

$$\gamma(0) = \gamma_0 \qquad \dot{\gamma}(0) = \dot{\gamma}_0$$

The aerodynamic coefficients C_{jk} and S_{jk}, written as such for convenience, correspond to the more conventional nomenclature[2] as follows: $C_{00} \sim C_l(\delta_A)$, $C_{10} \sim C_{lp}$, $C_{30} \sim C_{lp}{}^3$, $S_{01} \sim$ induced roll moment amplitude, etc. Finite upper bounds for the indices are chosen for the fitting process as required by the apparent degree of nonlinearity of the data; these are denoted J and K for the sums over j and k, respectively.

Standard Nonlinear Least Squares

Classical methods for applying least squares principles to differential equations are well known.[7,8] The basic procedure, similar to that required to fit an analytic function to data, requires the variation of the sum of the squares of the residuals with the perturbed coefficients to vanish; this leads to an iterative process for determining increments in the coefficients until some convergence criteria, usually on the sum of the squares of the residuals, is achieved.

The equations required for least squares application to Eq. (1) are summarized below.

The parameter set, $\bar{X}$, is given by

$$\bar{X}^T = [C_{00}, \ldots, S_{00}, \ldots]$$

The corrections to a trial set are given by

$$\Delta\bar{X} = \bar{B}^{-1}\bar{b} \tag{2}$$

where

$$\bar{B} = \bar{A}^T\bar{A}$$

$$\bar{b} = \bar{A}^T[\bar{\gamma}_{\text{obs}} - \bar{\gamma}(\bar{X})]$$

Here, $\bar{\gamma}_{\text{obs}}$ is the set of observations. Thus

$$\bar{\gamma}_{\text{obs}}{}^T = [\gamma(t_1), \gamma(t_2), \ldots]$$

Similarly $\bar{\gamma}(\bar{X})$ is the set of γ's computed for these times $(t_1, t_2 \ldots)$ for the trial parameters, $\bar{X}$. The rectangular matrix, $\bar{A}$, is

$$\bar{A} = \frac{\partial\bar{\gamma}}{\partial\bar{X}^T} = \begin{bmatrix} \dfrac{\partial\gamma_1}{\partial X_1} & \dfrac{\partial\gamma_1}{\partial X_2} & \cdots \\ \dfrac{\partial\gamma_2}{\partial X_1} & \dfrac{\partial\gamma_2}{\partial X_2} & \cdots \\ \vdots & \vdots & \end{bmatrix}$$

The required partial derivatives for solution of Eq. (2) are found from the simultaneous integration of

$$\ddot{\gamma} = \mathbf{Q} \sum_{j=0}^{J} \left(\frac{\dot{\gamma} d}{2V}\right)^j \sum_{k=0}^{K} (C_{jk} \cos 4k\gamma + S_{jk} \sin 4k\gamma) \tag{3}$$

$$\gamma(0) = \gamma_0 \qquad \dot{\gamma}(0) = \dot{\gamma}_0$$

$$\ddot{\bar{A}} = E\dot{\bar{A}} + F\bar{A} + \bar{G}$$

$$\bar{A}(0) = \bar{A}_0 \qquad \dot{\bar{A}}(0) = \dot{\bar{A}}_0$$

where

$$\bar{A}^T = \left[\frac{\partial\gamma}{\partial X_1} \frac{\partial\gamma}{\partial X_2} \cdots\right]$$

$$E = \mathbf{Q}\left(\frac{d}{2V}\right) \sum_{j=1}^{J} j \left(\frac{\dot{\gamma} d}{2V}\right)^{j-1} \sum_{k=0}^{K} (C_{jk} \cos 4k\gamma + S_{jk} \sin 4k\gamma)$$

$$F = 4\mathbf{Q} \sum_{j=0}^{J} \left(\frac{\dot{\gamma} d}{2V}\right)^j \sum_{k=1}^{K} k(-C_{jk} \sin 4k\gamma + S_{jk} \cos 4k\gamma)$$

$$\bar{G}^T = \left[\ldots \mathbf{Q}\left(\frac{\dot{\gamma} d}{2V}\right)^j \cos 4k\gamma \ldots \mathbf{Q}\left(\frac{\dot{\gamma} d}{2V}\right)^j \sin 4k\gamma \ldots, 00\right]$$

Equation (2), using Eq. (3), is solved for $\Delta\bar{X}$, the initial conditions and aerodynamic coefficients updated by $\Delta\bar{X}$ and the process repeated until some convergence criterion is satisfied.

Equation (2) is derived assuming that the best estimates for the initial conditions and aerodynamic coefficients are sufficiently close to the true values that $\Delta\bar{X}$ is small; this allows terms of order $\Delta\bar{X}^2$ to be neglected in a Taylor series expansion of $\bar{\gamma}$ about the best estimates. This fact, combined with the characteristics of the roll angular data and limited knowledge of several aerodynamic coefficients, generally allows the sum of the squares of the residuals to become excessively large during the fitting process and divergent corrections result. It is, therefore, necessary to consider an alternate application of these procedures to handle the rolling motion of finned bodies at large angles of attack.

Global Nonlinear Least Squares

The global application[9] of a least squares fit of Eq. (1) to observed data consists of segmenting the data in a desired manner and carrying out the fit in two phases: 1) maintaining constant (initial best estimates) values of the aerodynamic coefficients, "locally" fit each segment, j, independently for the initial conditions, γ_{oj} and $\dot{\gamma}_{oj}$, of that segment; and 2) "globally" fit all segments for one set of aerodynamic coefficients and n pairs of initial conditions.[13]

The philosophy in allowing jumps in γ and $\dot{\gamma}$ across segments is as follows. The real motion is driven mainly by the truncated series of terms for which coefficients are estimated. But there are additional terms of higher order which are neglected; there is also system noise such as turbulence and transients in the wind-tunnel incident stream. Due to these unmodeled torques and the singular sensitivity of the motion in the phase plane near saddle points, it is impossible to fit the motion continuously with only the modeled torque terms. The jumps across segments permit the motion to be accommodated to the truncated description of the applied torque. A more satisfying method of meeting the same objective may be to admit random torques with appropriate serial correlation statistics. This is the so-called "process noise" in Kalman filtering.

The local segment fitting is accomplished by solving equations very similar to Eq. (2), with only the increments of initial conditions to be determined. Consider the parameter set, $\bar{X}$, partitioned into sets

$$\bar{X}^a = \text{aerodynamic coefficients}$$

and

$$\bar{X}^j = \begin{pmatrix} \gamma_{0_j} \\ \dot{\gamma}_{0_j} \end{pmatrix} = \text{initial conditions for the } j\text{th segment}$$

$$\bar{X}^T = [\bar{X}^{a^T}, \bar{X}^{1^T}, \bar{X}^{2^T}, \ldots \bar{X}^{j^T}, \ldots]$$

Equation (2), with Eq. (3), may therefore be employed to obtain $\Delta\bar{X}^j$, where $\bar{X}^a$ is held fixed at the initial best estimates. The set

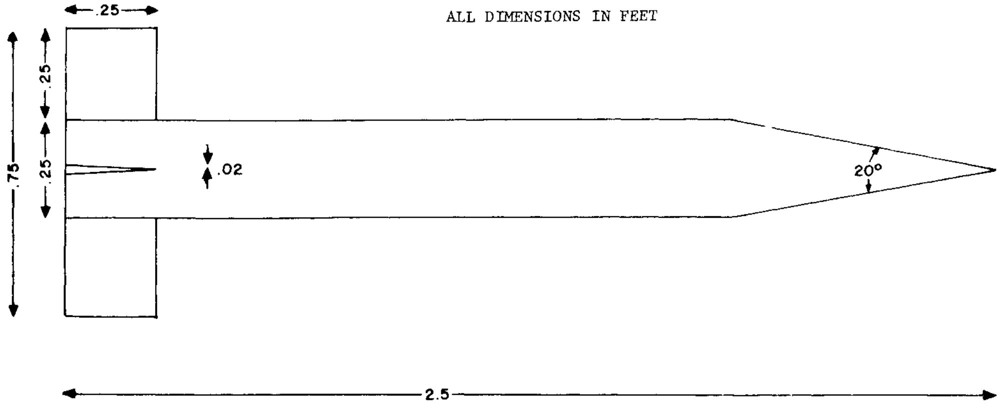

Fig. 2 Schematic of basic research configuration.

of observations for each segment, j, are employed in the solution of these equations. That is, γ_{obs} is partitioned as

$$\bar{\gamma}_{obs}^{T} = [\bar{\gamma}_{obs}^{1^T}, \bar{\gamma}_{obs}^{2^T}, \ldots \bar{\gamma}_{obs}^{j^T} \ldots]$$

Upon achieving convergence on n (equal to the number of segments) pairs of initial conditions, the global fit is made by solving for increments in the n pairs of initial conditions and $J \cdot K$ values of the aerodynamic coefficients as follows:

$$\Delta \bar{X} = \bar{B}^{-1}\bar{b} \tag{4}$$

where

$$\bar{B} = \begin{bmatrix} \bar{B}^{aa} & \bar{B}^{a1} & \bar{B}^{a2} & \bar{B}^{a3} & \ldots \\ \bar{B}^{1a} & B^{11} & 0 & 0 & \ldots \\ \bar{B}^{2a} & 0 & \bar{B}^{22} & 0 & \ldots \\ \bar{B}^{3a} & 0 & 0 & \bar{B}^{33} & \\ - & - & - & - & - \\ - & - & - & - & - \end{bmatrix}$$

$$\bar{b}^{T} = [\bar{b}^{a^T}, \bar{b}^{1^T}, \bar{b}^{2^T}, \ldots \bar{b}^{j^T} \ldots]$$

$$\bar{b}^{a} = \sum_{j} \{\bar{A}^{a^T}[\bar{\gamma}_{obs}^{j} - \bar{\gamma}^{j}(\bar{X})]\}$$

$$\bar{b}^{j} = \bar{A}^{j^T}[\bar{\gamma}_{obs}^{j} - \bar{\gamma}^{j}(\bar{X})]$$

Here $\bar{\gamma}_{obs}^{j}$ and $\bar{\gamma}^{j}(X)$ are the observed and computed sets of γ for the jth segment, respectively. In addition

$$\bar{A}^{j} = \frac{\partial \bar{\gamma}}{\partial(\gamma_{j_0}, \dot{\gamma}_{j_0})} = \begin{bmatrix} \dfrac{\partial \gamma_1^{j}}{\partial \gamma_0^{j}} & \dfrac{\partial \gamma_1^{j}}{\partial \dot{\gamma}_0^{j}} \\ \dfrac{\partial \gamma_2^{j}}{\partial \gamma_0^{j}} & \dfrac{\partial \gamma_2^{j}}{\partial \dot{\gamma}_0^{j}} \\ -- & -- \\ -- & -- \end{bmatrix}$$

$$\bar{A}^{a} = \frac{\partial \bar{\gamma}}{\partial \bar{X}^{a^T}}$$

$$\bar{B}^{aj} = \bar{A}^{a^T}\bar{A}^{j}$$

$$\bar{B}^{aa} = \bar{A}^{a^T}\bar{A}^{a}$$

$$\bar{B}^{jj} = \bar{A}^{j^T}\bar{A}^{j}$$

$$\bar{B}^{jk} = 0 \text{ if } j \neq k$$

The required partial derivatives for solution of Eq. (4) are obtained from solution of Eq. (3). The increments in initial conditions for each segment and the aerodynamic coefficients are added to the first best estimates, and Eqs. (3) and (4) are solved in an iterative fashion until convergence is achieved. The techniques employed for determining initial estimates of aerodynamic coefficients and initial conditions of each segment are discussed in Ref. 10.

Experimental Data

The roll angular data discussed in this paper was obtained from subsonic wind tunnel tests[11] of the configuration shown in Fig. 2 in pure rolling motion. The tests were conducted in the Naval Ship Research and Development Center's 7 × 10-ft. subsonic wind tunnel at a freestream velocity of 117 fps. The dynamic pressure during the tests was approximately 16.3 lb/ft^2 with a Reynolds number of approximately 7.5×10^5/ft.

During the tests, the model was held at constant angle of attack and supported on an air bearing in order to be free to roll. Measurements of roll angle as a function of time were made using a high speed movie camera. The model has a positive (inducing clockwise spin, viewed from the rear) fin cant of 1° in all tests. Data at 57° angle of attack are presented and analyzed in this paper. Roll angular data at other angles of attack are discussed in Ref. 11; similar analyses of test data at 45° and 66° angle of attack are presented in Ref. 12. Figures 3 and 4 show plots of roll angle vs camera frame number of this angle of attack. The correlation between camera frame number and

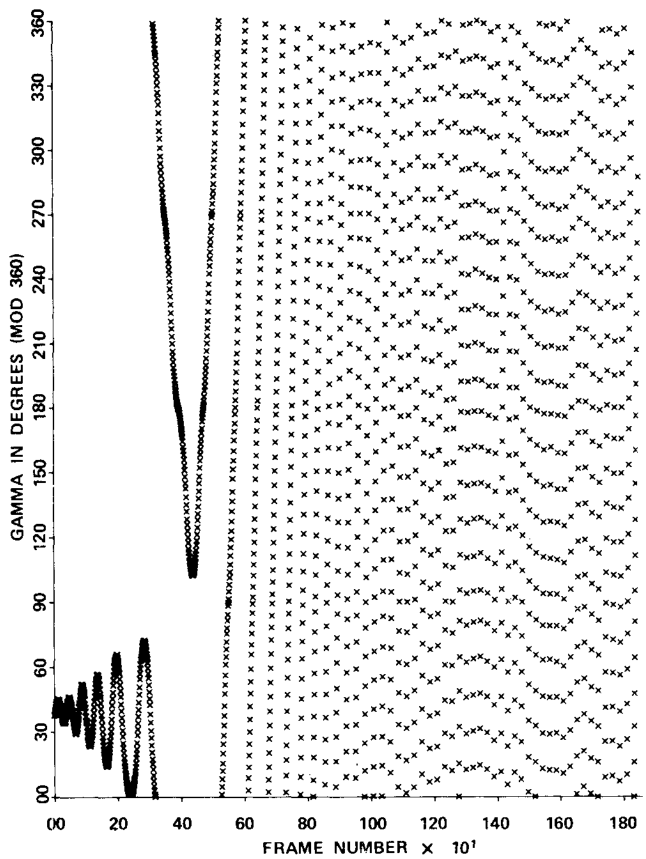

Fig. 3 Experimental roll angular data ($\alpha = 57°$, run 1).

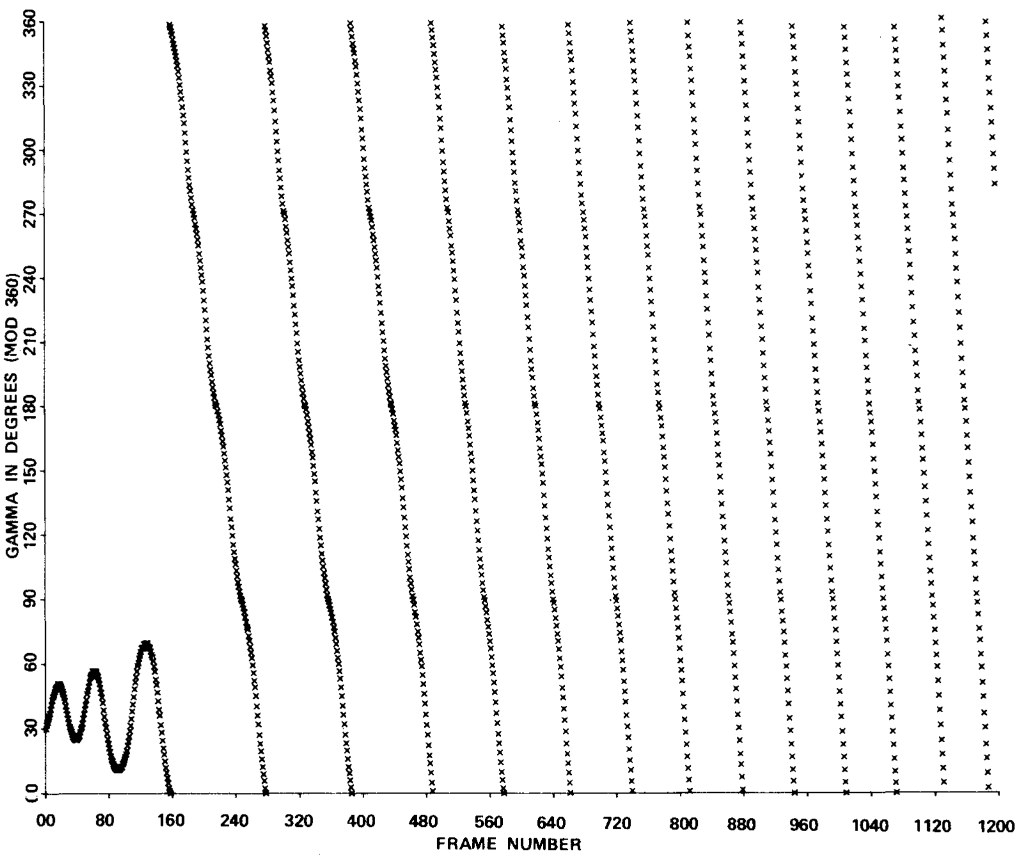

Fig. 4 Experimental roll angular data (α = 57°, run 2).

time is evident from Figs. 5 and 6. Roll angle is plotted on a scale from 0° to 360° to limit the plots to a usable size.

The different types of motion observed during the tests are discussed in detail in Ref. 11. It was found by phase plane analysis that in order to obtain some of the dynamic roll behavior seen in these tests, it was necessary that small aerodynamic and/or mass asymmetry terms be considered in the analysis. This, combined with the fact that the wind-tunnel model possessed some degree of asymmetry, leads to the following modification to Eq. (1):

$$\ddot{\gamma} = \mathbf{Q} \sum_{j=0}^{J} \left(\frac{\dot{\gamma} d}{2v}\right)^{j} \sum_{k=0}^{K} (C_{jk} \cos 4k\gamma + S_{jk} \sin 4k\gamma) + C_{a_c} \cos\gamma + C_{a_s} \sin\gamma \qquad (5)$$

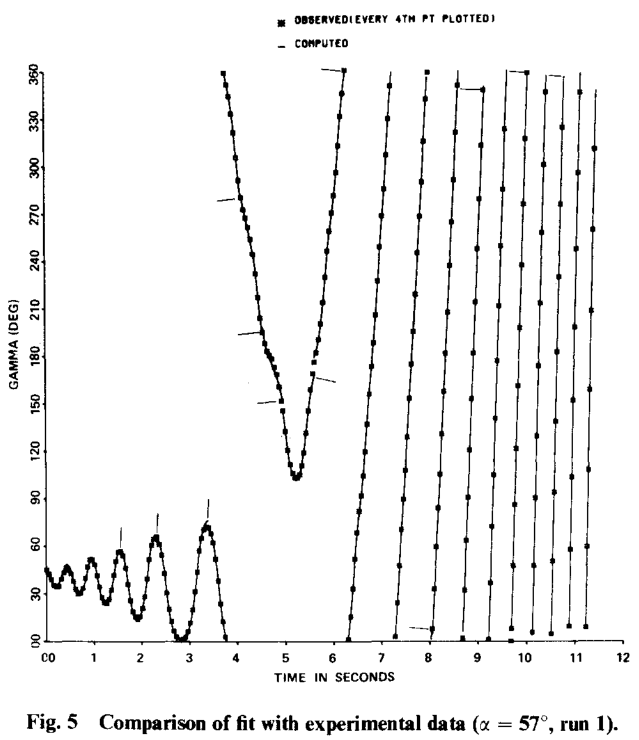

Fig. 5 Comparison of fit with experimental data (α = 57°, run 1).

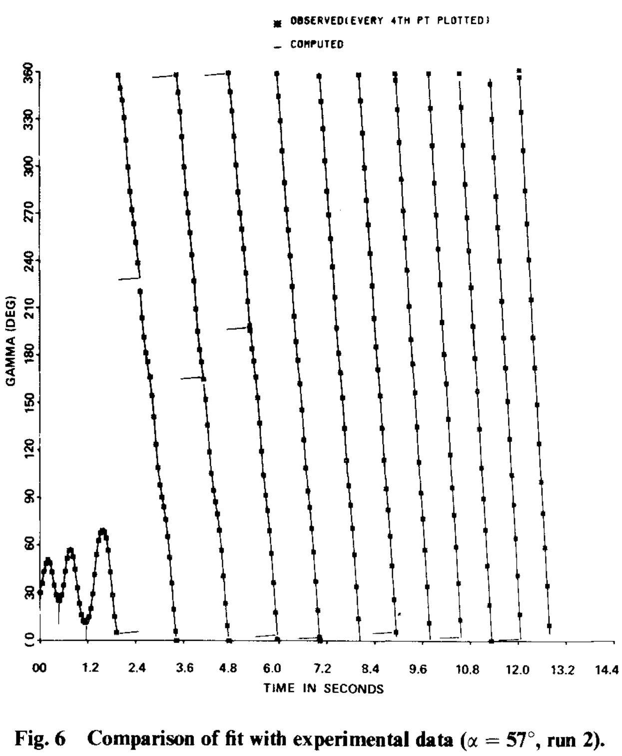

Fig. 6 Comparison of fit with experimental data (α = 57°, run 2).

Table 1 Aerodynamic coefficients considered in fits

Coefficient	Description
S_{01}, S_{02}, S_{03}, S_{04}, S_{05}	Induced (static) roll Moment coefficients (skew symmetric)
C_{00}	Basic fin cant moment coefficient
C_{01}, C_{02}	Variation of fin cant moment coefficient with roll angle (symmetric)
C_{10}	Linear roll damping moment coefficient
C_{11}, C_{12}	Variation of linear roll damping moment coefficient with roll angle
C_{30}	Cubic roll damping moment coefficient
C_{ac}, C_{as}	Asymmetry roll coefficients

where C_{a_c} and C_{a_s} are the added asymmetry terms. The equations discussed previously describing the global fitting process may be extended in a straightforward manner to include the additional terms.

A characteristic of nonlinear systems is the dependence of the steady-state motion on initial conditions. Referring to Figs. 5 and 6, it is seen that the resulting roll speed-up and steady-state spin occurred in opposite directions for different initial roll angles and angular velocities. A similar occurrence was observed in the data of 66° angle of attack.[11,12]

Discussion of Results

Twelve aerodynamic coefficients (plus the two asymmetry terms) were considered in fitting the data; a summary is presented in Table 1. The fitting process for a particular set of data was initiated by using small segment sizes (i.e., a large number of segments) and a limited number of coefficients. In the oscillating portions of the data, segments were initially chosen to include 1 cycle of oscillation, with the segments beginning at the peaks (zero roll rate points) of each cycle. Very small segment sizes were also used where pronounced saddle point effects (significantly reduced roll rate) appeared. In the roll speed-up and steady-state spin portions of the data, larger segment sizes could be used; segments were generally chosen to include 180° of roll in roll speed-up regions and 360° in steady-state spin. Generally speaking, residual biases in each or all the segments were used as indicators regarding the length of the segments or the number of aerodynamic coefficients considered. Heavy biases in all segments implied the need for more aerodynamics, while a heavy bias in selected segments implied the need for shortening the corresponding segment. The coefficients generally used to begin the fitting process for a data set were S_{01}, C_{00}, C_{10}, C_{11}, C_{30}, C_{ac}, and C_{as}.

Table 2 Aerodynamic coefficient values and standard deviations ($\alpha = 57°$)

Coefficient	Value (c)	Standard deviation (σ_c)	Signal/noise (c/σ_c)
S_{01}	0.88522	0.00105	840.3
S_{02}	−0.15763	0.00144	110.6
S_{03}	0.14640	0.00182	80.5
S_{04}	−0.04077	0.00243	16.8
S_{05}	0.04751	0.00249	19.1
C_{00}	0.03010	0.00006	502.5
C_{01}	0.30695	0.00112	274.0
C_{02}	−0.07565	0.00159	47.6
C_{10}	4.7992	0.01855	258.4
C_{11}	−25.134	0.25028	100.4
C_{12}	40.287	0.77884	51.7
C_{30}	−7493.7	74.530	100.5
C_{ac}	−0.10675	0.00031	344.8
C_{as}	−0.04478	0.00032	140.0

Having obtained a fit with the reduced set of coefficients and small segment sizes, the remaining coefficients were added (in increments of 3 or 4) until the data was fit with the final set of aerodynamics. The data were then refit with increasing segment sizes until the resulting set of coefficients would produce a phase plane exhibiting the general characteristics of the motion observed in the data. During the fitting process it was found that individual segments should include more than 1 cycle of oscillatory data in order to adequately determine linear damping coefficients.

Initially, each set of data shown in Figs. 3 and 4 was fit independently for a set of aerodynamics. Later, both data runs were combined and fit together for one set of aerodynamics. This procedure was also followed for data at other angles of attack (45° and 66°) not discussed in this paper.[12] Static roll moments obtained from these combined fits closely agreed with those obtained from the individual data set which contained the most oscillations before roll break-out. For this reason, and the fact that linear damping coefficients are better determined from oscillatory data, experimental roll angular data should contain as many cycles as possible preceding roll break-out and speed-up.

The strength of the aerodynamic solution was examined through the formal variance-covariance matrix. This is the "aerodynamic block" $(\bar{B}^{-1})^{aa}$, of the inverse normal matrix, $\bar{B}^{-1}$, properly weighted for the variance in the observations σ_γ^2. Note that σ_γ was found from difference tables of γ to be approximately 0.25°. The formal standard deviation of the jth aerodynamic coefficient is

Table 3 Correlation coefficients ($\alpha = 57°$)[a]

Coeff.	S_{01}	S_{02}	S_{03}	S_{04}	S_{05}	C_{00}	C_{01}	C_{02}	C_{10}	C_{11}	C_{12}	C_{30}	C_{ac}	C_{as}
S_{01}	1.0	0.037	−0.004	0.116	−0.117	−0.139	0.059	0.295	−0.017	0.149	0.085	0.022	−0.186	−0.141
S_{02}		1.0	0.338	0.073	0.162	−0.135	−0.114	−0.195	0.094	0.046	0.179	−0.032	−0.180	−0.226
S_{03}			1.0	0.181	0.104	−0.123	−0.163	−0.131	0.165	0.114	−0.238	−0.068	−0.144	−0.146
S_{04}				1.0	−0.292	−0.036	−0.010	−0.200	−0.028	0.041	0.319	0.017	−0.080	−0.043
S_{05}					1.0	−0.025	−0.212	−0.219	−0.041	−0.094	−0.064	0.021	−0.091	0.017
C_{00}						1.00	0.168	0.037	0.104	−0.095	−0.009	−0.161	0.291	0.072
C_{01}							1.00	0.092	0.042	0.075	0.190	−0.036	0.332	0.287
C_{02}								1.0	−0.035	−0.022	−0.219	0.014	0.065	0.082
C_{10}									1.0	0.840	0.230	−0.696	0.134	−0.033
C_{11}										1.0	0.427	−0.422	0.120	−0.082
C_{12}											1.0	−0.115	0.058	−0.031
C_{30}												1.00	−0.077	0.0001
C_{ac}													1.0	0.175
C_{as}														1.0

[a] Matrix is symmetric.

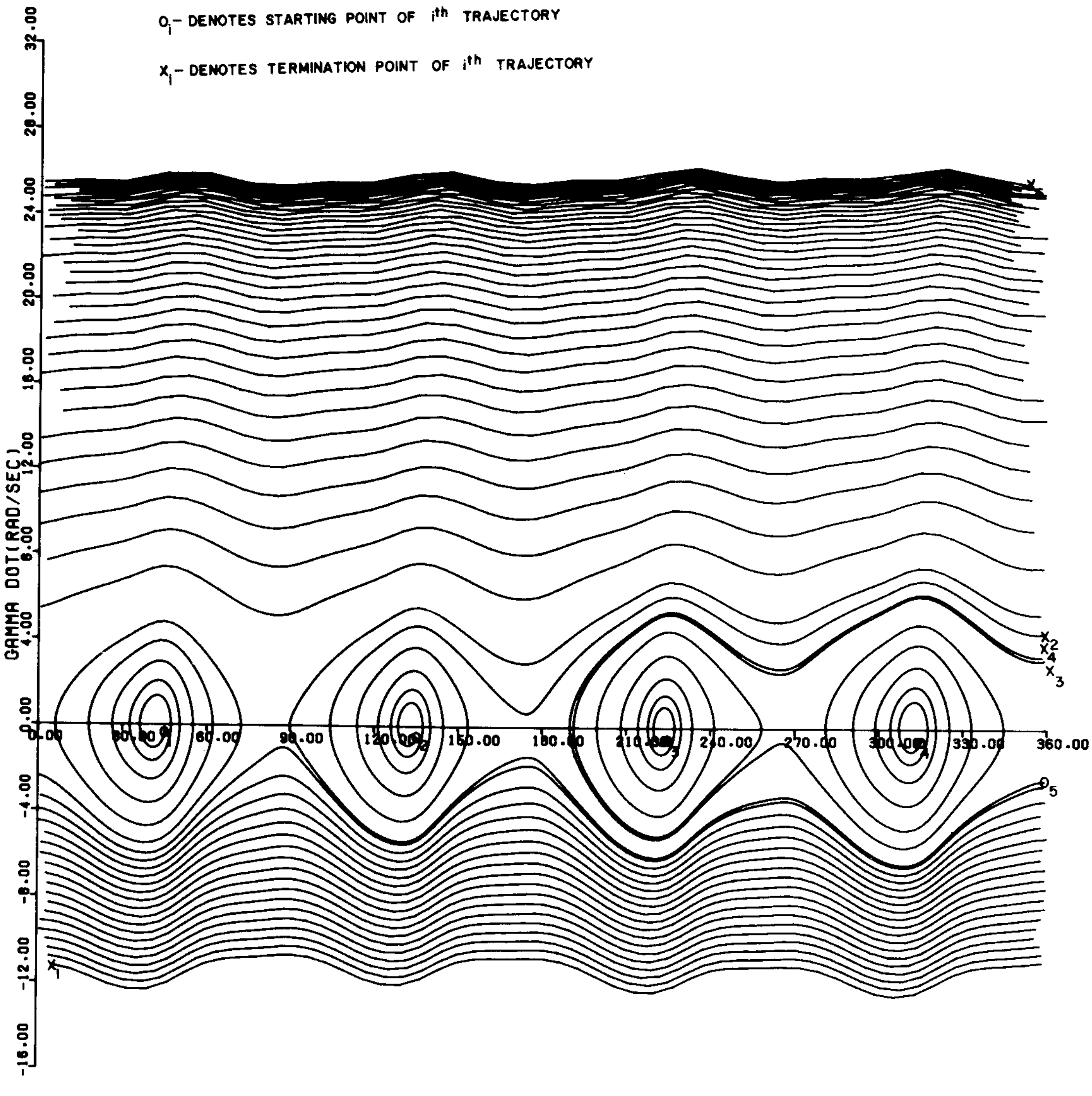

Fig. 7 **Rolling motion phase plane ($\alpha = 57°$).**

$$\sigma_i = [(\bar{B}^{-1})^{aa}_{ii}]^{1/2}\sigma_\gamma$$

and the correlation coefficient between the ith and jth coefficient is

$$\rho_{ij} = \left[\frac{(\bar{B}^{-1})^{aa2}_{ij}}{(\bar{B}^{-1})^{aa}_{ii}(\bar{B}^{-1})^{aa}_{jj}}\right]^{1/2}$$

Values for the aerodynamic coefficients (c_i) as well as σ_i and ρ_{ij}, for the data analyzed are presented in Tables 2 and 3. The high formal signal/noise ratios (c_i/σ_i) and the modest correlation coefficients indicate a very strong solution. The strength is valid only provided the truncated aerodynamic series has a negligible remainder.

The fits to the data were found to possess maximum bias and rms residual signal in a given segment of approximately 0.5° and 2°, respectively. The average bias and rms residual signal for all data segments and angles of attack[12] were 0.13° and 1.2°, respectively. The residuals showed rather solid runs of sign on the order of 0.1 sec (approximately 10 observations) with a maximum run of 0.6 sec.

These features, viz., 1) large formal signal to noise ratio, 2) significant residual bias and variance (relative to the observed variance), and 3) the runs of sign in the residuals, suggest that there are still more aerodynamics which could be extracted from the data.

Figures 5 and 6 show comparisons of observed and computed values of roll angle for $\alpha = 57°$. The lines normal to the computed curves in these figures indicate segment locations for the fits. Computed values of roll angle were obtained using the aerodynamic coefficients in Table 2, i.e., those obtained by combining data sets at the same angle of attack. As can be seen from the figures as well as the residual statistics given above, excellent agreement with observed data was obtained.

A phase plane ($\dot{\gamma}$ vs γ) generated by integrating Eq. (5) using the aerodynamics of Table 2 and for several initial conditions is shown in Fig. 7 for an angle of attack of 57°. The phase plane exhibits the general characteristics of the motion observed in the experimental data. The impact of asymmetries on observed roll behavior is discussed in light of phase plane behavior in Ref. 12.

Various roll moment coefficients can be computed from the aerodynamics given in Table 1. These data, including the variation of induced roll, fin cant and roll damping moments with roll angle, are summarized in Ref. 12. Comparison of induced roll moment extracted from dynamic data with that obtained by strain gage[6] is also discussed.

Experimental data at 57° angle of attack (as well as that at 66° angle of attack[12]) showed roll speed-up in both positive and negative directions. This type of motion has been shown[6]

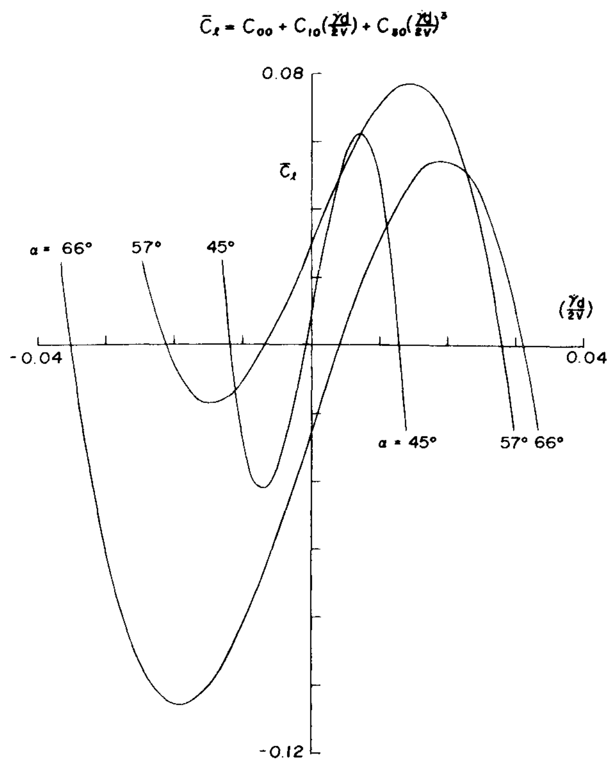

Fig. 8 Average roll moment coefficient, $\bar{C}_l$, vs nondimensional spin, $\dot{\gamma}d/2v$.

to require an average (over 360° of roll) roll damping coefficient at least cubic in $\dot{\gamma}$. Neglecting variations with roll angle, which are small near (high) steady-state spin, the average roll moment coefficient is

$$\bar{C}_l = C_{00} + C_{10}(\dot{\gamma}d/2v) + C_{30}(\dot{\gamma}d/2v)^3$$

Figure 8 shows $\bar{C}_l$ vs nondimensional spin $(\dot{\gamma}d/2v)$ for three angles of attack. Stable steady-state spin rates occur where $\bar{C}_l = 0$ and $\partial\bar{C}_l/\partial(\dot{\gamma}d/2v) < 0$. Figure 8 shows the increasing magnitude of steady-state spin rate as the angle of attack is increased from 45° to 66°. The effect of fin cant (C_{00}) on the relative magnitudes of positive and negative steady-state spin rates at each angle of attack is also shown.

Summary

A method has been presented for analyzing and predicting the (nonlinear) rolling motion of finned missiles at high (and low) angles of attack. "Global" nonlinear least squares procedures were applied to the differential equation describing the nonlinear rolling motion of finned missiles to extract pertinent aerodynamic coefficients. The technique was applied to highly nonlinear, experimental roll angular data taken on a basic research configuration at an angle of attack of 57°. The method was shown to be capable of determining aerodynamic coefficients describing the rolling motion at these high angles of attack. Extracted aerodynamics for this angle of attack were presented, and the impact of specific coefficients on observed motion was discussed.

In applying the technique, several trends were observed which led to general conclusions concerning the optimum characteristics of the experimental data. Static roll moment coefficients and linear roll damping coefficients were better determined from oscillatory data; cubic damping coefficients could only be determined from roll speed-up and steady-state spin data. Therefore, experimental roll angular data to be used in conjunction with the "global" fitting technique should contain several cycles of roll oscillations prior to roll break-out. The data should also include roll speed-up and steady-state spin, preferably in both positive and negative directions, at each angle of attack. It is inferred that there is appreciably more aerodynamic information which could be extracted from the present data if the series were truncated farther out. Further work is planned in this area. In addition, the technique will be extended to allow analysis of rolling motion in the presence of pitching and yawing motion (i.e., variable angle-of-attack effects).

References

[1] Nicolaides, J. D., "An Hypothesis for Catastrophic Yaw," TN-18, 1955, Bureau of Ordnance, U.S. Navy, Washington, D.C.

[2] Nicolaides, J. D., "Missile Flight and Aerodynamics," TN-100-A, 1961, Bureau of Naval Weapons, Washington, D.C.

[3] Daniels, P., "Fin Slots vs Roll Lock-In and Roll Speed-Up," *Journal of Spacecraft and Rockets*, Vol. 4, No. 3, March 1967, pp. 410–412.

[4] Nicolaides, J. D. and Bolz, R. E., "On the Pure Rolling Motion of Winged and/or Finned Missiles in Varying Supersonic Flight," BRL Rept. 799, 1952, Ballistics Research Labs., Aberdeen Proving Ground, Md.

[5] Regan, F. J., "Roll Damping Moment Measurements for the Basic Finner at Subsonic and Supersonic Speeds," Rept. 6652, June 1964, Naval Ordnance Lab., White Oak, Silver Spring, Md.

[6] Daniels, P., "A Study of the Nonlinear Rolling Motion of a Four-Finned Missile," *Journal of Spacecraft and Rockets*, Vol. 7, No. 4, April 1970, pp. 510–512.

[7] Chapman, G. T. and Kirk, D. B., "A Method for Extracting Aerodynamic Coefficients from Free Flight Data," *AIAA Journal*, Vol. 8, No. 4, April 1970, pp. 753–758.

[8] Chapman, G. T. and Kirk, D. B., "Aerodynamics of Bodies from Motion Analysis," AGARDograph 138, 1970, pp. 267–348.

[9] Sheffield, C. and Morris, J. P., "Organization of a Large Scale Computer Program for Space Age Geodesy," NWL TR-1990, July 1965, Naval Weapons Lab., Dahlgren, Va.

[10] Cohen, C. J. and Clare, T. A., "Analysis of the Rolling Motion of Finned Missiles at Large Angles of Attack," NWL TR-2671, Feb. 1972, Naval Weapons Lab., Dahlgren, Va.

[11] Stevens, F. L., "Subsonic Wind Tunnel Tests of the Basic Finner Missile in Pure Rolling Motion," NWL TN-K-4/72, Feb. 1972, Naval Weapons Lab., Dahlgren, Va.

[12] Cohen, C. J., Clare, T. A., Stevens, F. L., "Analysis of the Rolling Motion of Finned Missiles," AIAA Paper 72-980, Palo Alto, Calif., 1972.

[13] Reynolds, J. H., "ROMOF: A CDC 6700 Computer Program for Fitting Rolling Motion Data of Cruciform-Finned Missiles," NWL TN-K-42/73, July 1973, Naval Weapons Lab., Dahlgren, Va.